Pergamon

Cement and Concrete Research 29 (1999) 1663–1671

CEMENT AND CONCRETE RESEARCH

Effects of cement particle size distribution on performance properties of Portland cement-based materials

Dale P. Bentz[a,*], Edward J. Garboczi[a], Claus J. Haecker[b], Ole M. Jensen[c]

[a]*Building and Fire Research Laboratory, Building 226 Room B-350, National Institute of Standards and Technology, Gaithersburg, MD 20899, USA*

[b]*Wilhelm Dyckerhoff Institut, Wiesbaden, Germany*

[c]*Technical University of Denmark, Lyngby, Denmark*

Received 12 April 1999; accepted 14 July 1999

Abstract

The original size, spatial distribution, and composition of Portland cement particles have a large influence on hydration kinetics, microstructure development, and ultimate properties of cement-based materials. In this paper, the effects of cement particle size distribution on a variety of performance properties are explored via computer simulation and a few experimental studies. Properties examined include setting time, heat release, capillary porosity percolation, diffusivity, chemical shrinkage, autogenous shrinkage, internal relative humidity evolution, and interfacial transition zone microstructure. The effects of flocculation and dispersion of the cement particles in the starting microstructures on resultant properties are also briefly evaluated. The computer simulations are conducted using two cement particle size distributions that bound those commonly in use today and three different water-to-cement ratios: 0.5, 0.3, and 0.246. For lower water-to-cement ratio systems, the use of coarser cements may offer equivalent or superior performance, as well as reducing production costs for the manufacturer.

Keywords: Cement paste; Hydration; Modeling; Particle size distribution; Transport properties

1. Introduction

Many studies have been conducted examining the relationships between Portland cement particle size distribution (PSD) and the hydration kinetics and hardened paste strength properties [1–6]. For a given water-to-cement (w/c) ratio, a reduction in median particle size generally results in an increased hydration rate and, therefore, improved early properties such as higher early strengths. For this reason, Portland cement finenesses have generally increased over the years. However, Mehta [7] has pointed out that for durability considerations, finer cements may not always be preferable to coarser ones. Furthermore, it has recently been argued that in high-performance concretes with relatively low w/c ratios, coarser cements may offer equivalent long-term performance to finer cements [8], resulting in energy savings due to a reduction in grinding time. This conclusion was based on simulation studies of the degree of hydration vs. time behavior of a set of cements ground to different finenesses. The purpose of this paper is to extend that study to investigate a wide range of properties for two cement finenesses (640 and 210 m^2/kg) significantly different from the cement fineness of about 350 to 400 m^2/kg typically produced by the cement industry today.

2. Experimental and modeling approach

All simulations presented were conducted using the NIST microstructural model that has been described in detail elsewhere [9,10]. Based on a set of cellular automaton rules, the model operates on a three-dimensional digitized microstructure consisting of a volume of pixel elements to simulate the reactions between cement and water. For the present study, the following modifications were made to the base model described elsewhere [10]. First, the reaction of hemihydrate to produce gypsum was included so that various forms of sulfate could be studied. Second, the dissolution algorithm was changed so that the 12 next-nearest neighbor pixels (in three-dimensional view), in addition to the six immediate neighbors, are considered as possible dissolution sites. This modification increases the long-term degree of hydration of the larger (diameter > 10 μm) cement particles in the model cements. Finally, the induction period was incorporated into the NIST model for the first time in a simple manner by making the "early-age" dissolution prob-

* Corresponding author. Tel.: 301-975-5865; fax: 301-990-6891.
E-mail address: dale.bentz@nist.gov (D.P. Bentz)

0008-8846/99/$ – see front matter
PII: S0008-8846(99)00163-5

abilities of the cement phases proportional to the formation of one of the reaction phases, the C-S-H gel. Specifically, while the volume fraction of C-S-H gel formed is less than 0.07, the dissolution probabilities of all cement phases (aluminates included) are multiplied (and thus reduced) by a factor equal to the current volume fraction of C-S-H divided by 0.07. This factor was selected to provide good agreement with isothermal calorimetry data on the hydration of pure C_3S obtained at temperatures ranging from 10 to 40°C [11]. While several induction period mechanisms have been developed and advanced [6], the hypothesis gaining support most recently is that the induction period is controlled by the nucleation and growth of the C-S-H gel phase [12]. This simple dissolution rule will produce an autoacceleratory reaction, which will decay at longer times due only to spatial effects, as further hydration becomes impeded by the previously produced hydration products.

The microstructural model has been developed to operate under a variety of curing conditions (water-saturated, sealed, etc.). For this study, to simulate well-cured systems, all hydration simulations were executed under saturated conditions until the capillary porosity depercolated, at which point all subsequent hydration was executed under sealed (no further water ingress) curing conditions [13]. Once the model switches to sealed conditions, the necessary empty porosity, corresponding to the chemical shrinkage caused by hydration, is automatically created [13]. Current research is focused on the incorporation of a drying algorithm into the NIST cement hydration model, so that a wider variety of curing conditions and their durability implications may be quantitatively explored.

The model was used to simulate the experimentally observed hydration behavior of two cements of vastly different finenesses made from the same clinker [8]. Laser diffraction techniques were used to determine the PSD of each of the dry cement powders, and quantitative X-ray diffraction was applied to determine the fraction of tricalcium silicate (C_3S) that had reacted at ages of 1, 2, 3, 4, 7, 14, 28, and 56 days for a w/c ratio = 0.5 cement paste. The cumulative PSDs measured for the two cements are shown in Fig. 1. The cement PSDs will be referred to as "5 μm" and "30 μm," proceeding from left to right in Fig. 1, corresponding approximately to their "average" size obtained by fitting them to a Rosin-Rammler distribution [6]. Ordinary ASTM Type I Portland cements commonly used today would fall somewhere between these two curves, but would in general lie closer to the curve on the left. The composition of the cement (more typical of an ASTM Type V, low C_3A cement), determined by quantitative optical microscopy and subsequent point sampling (5,000 points), is 59% C_3S, 25.9% C_2S, 0.6% C_3A, and 14.2% C_4AF, with hemihydrate added at a mass percentage of 4.6%.

The measured PSDs and clinker compositions were used in constructing the initial model microstructures for cement pastes with w/c ratios of 0.246, 0.3, and 0.5. The calculations for the w/c = 0.5 model runs were used as a baseline,

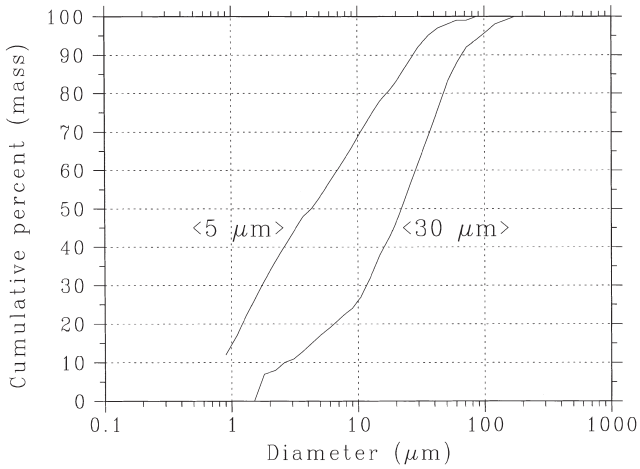

Fig. 1. Measured particle size distributions for the two Portland cements.

because experimental quantitative X-ray diffraction measurements of the degree of hydration of the C_3S were performed at this w/c ratio [8]. These initial systems were hydrated using the NIST microstructural model to study the effects of PSD on hydration kinetics and the following properties: setting time, heat release, capillary porosity percolation, diffusivity, and chemical shrinkage. All hydrations were executed for 5,000 cycles of the model, corresponding to 25,000 h (about 3 years) of real time at 20°C. Generally, the cement particles were flocculated before hydration commenced. However, for the w/c = 0.5 systems, two additional microstructures consisting of dispersed cement particles (each particle separated from all neighbors by at least one pixel or 1 μm) were investigated. In a further set of simulations, a single, flat plate aggregate, two pixels thick, was added to the central portion of the 100 · 100 · 100-pixel microstructure prior to cement particle placement to quantitatively evaluate the effects of w/c ratio and cement PSD on interfacial transition zone microstructural development. This latter study was conducted for the w/c = 0.3 and 0.5 systems, for each of the two cement PSDs.

Percolation properties of total solids (set) and the capillary porosity phase were monitored periodically throughout the hydration process. Additionally, microstructures were output after 0, 100, 200, 300, 500, 1,000, 2,000, and 5,000 cycles of hydration for evaluation of diffusivities using a finite difference code developed by Garboczi [14]. For the diffusivity calculation, the empty and water-filled porosity pixels were assigned a relative diffusivity of 1 and the C-S-H gel pixels were assigned a value of 1/400 [15], with all remaining cement phase pixels being assigned a diffusivity of 0. The empty porosity was assigned a diffusivity of 1 based on the assumption that over time these pores will become saturated with water [16]. This assumption represents a worst case scenario, so that the computed relative diffusivities will be upper bounds.

3. Results and discussion

To calibrate the model to real time, one parameter that relates model cycles to time in an equation of the form: time (h) = $B \cdot \text{cycles}^2$ needs to be specified [9]. Based on the experimental measurements for w/c = 0.5 at 20°C for the 5-μm cement, B was set at a value of 0.001 h/cycle^2 (compared with previously used values of 0.0017 [9] and 0.0011 [17], both at 25°C). Using this factor, Fig. 2 provides a plot of the conversion of tricalcium silicate as a function of time for both the model and real systems. The agreement between model predictions and experimental observations is excellent, falling well within the relative standard uncertainty of 13% for the experimental measurements. This suggests that the model adequately describes the effects of PSD on hydration kinetics. It is clear from Fig. 2 that for w/c = 0.5, finer grinding results in increased hydration (and therefore enhanced strength) at all ages investigated in this study.

3.1. Setting time

The setting of cement is controlled by the formation of a network of partially hydrated cement particles connected by hydration products [12] that can resist a shear force. In the model, set is determined as the time or degree of hydration required to first form a percolated pathway through the three-dimensional microstructure consisting of cement particles connected to one another either by C-S-H gel or ettringite. Table 1 reports the results obtained for the three different w/c ratios and the two cement PSDs. Both hydration time and degree of hydration are reported to separate the effects of hydration kinetics from microstructural considerations. Thus, even though the finer cement requires less time to achieve set due to its increased hydration rate, it actually requires more hydration since more particle-to-particle bridges need to be built to form a percolated pathway.

Table 1
Setting properties of model cement pastes

w/c	PSD (μm)	Time of set (h)	Degree of hydration at set
0.246	5	0.58	0.020
0.246	30	0.90	0.011
0.3	5	0.78	0.025
0.3	30	1.44	0.016
0.5	5	1.44	0.074
0.5	30	3.36	0.036
0.5[a]	5	1.60	0.089
0.5[a]	30	4.76	0.055

[a]Dispersed system.

This simulation result is consistent with a set of rheological measurements [18], which indicated that for a C_3S cement with the smallest particles removed, less hydration was needed to achieve set than with the original C_3S cement. For the w/c = 0.5 systems, as shown in Table 1, executing the simulation for dispersed cement particles resulted in small increases in both the time and degree of hydration needed to achieve set, because more hydration is needed to link the particles when they are initially dispersed further apart. This microstructural observation may partially explain the retardation generally observed when using water-reducing agents or superplasticizers, in addition to any chemical effects these admixtures may produce. As the w/c ratio is increased, the difference in setting times between the 5- and 30-μm cements becomes more significant (several hours for w/c = 0.5 vs. about 30 min for the two lower w/c ratios).

3.2. Heat release

Naturally, the finer cement hydrates more rapidly, resulting in a higher initial rate of heat release as shown in Fig. 3. For w/c = 0.3 cement pastes, however, after 5,000 cycles of model hydration the cumulative degrees of hydration (Table

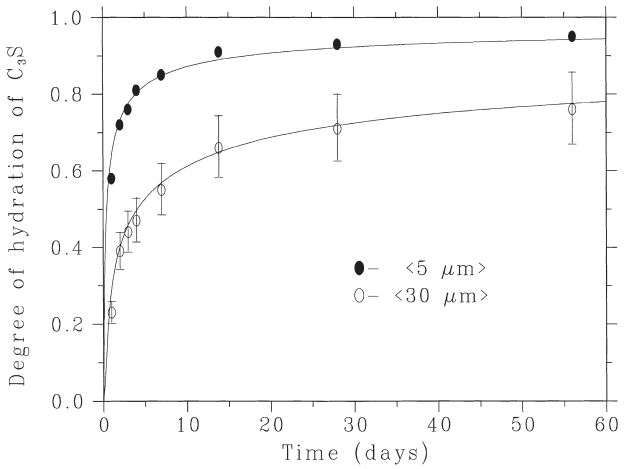

Fig. 2. Experimental (data points) and model (lines) results for degree of hydration of the C_3S phase for w/c = 0.5 at 20°C. Error bars for 30-μm data points indicate a relative standard uncertainty of 13% in all experimental measurements.

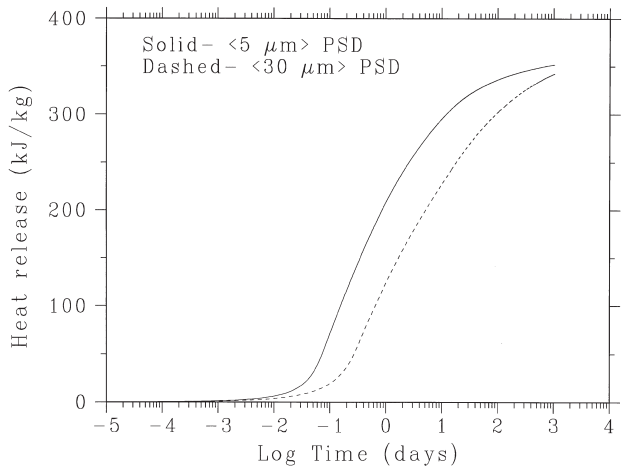

Fig. 3. Cumulative heat release for hydration under isothermal conditions for w/c = 0.3 model cement pastes.

Table 2
Porosity of model cement pastes after 5,000 cycles of hydration

w/c	PSD (μm)	Empty porosity fraction	Water-filled porosity fraction	Degree of hydration
0.246	5	0.037	0.0003	0.60
0.246	30	0.029	0.003	0.58
0.3	5	0.036	0.009	0.72
0.3	30	0.028	0.022	0.69
0.3[a]	30	0.075	0.013	0.62
0.5	5	0.013	0.166	0.95
0.5	30	0.000	0.228	0.83

[a]Totally sealed hydration.

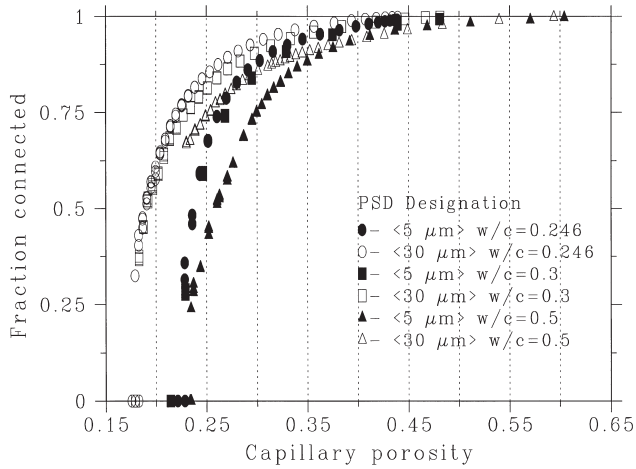

Fig. 4. Model results for capillary porosity percolation for cement pastes.

2) and heat released are nearly equivalent. For many applications, the avoidance of a rapid initial heat release is beneficial in limiting the development of thermal stresses and minimizing early-age cracking problems. Thus, this is one area where the use of a coarser cement may offer a performance benefit relative to a finer one. For the w/c = 0.5 cement pastes, even after 5,000 cycles of model hydration the degree of hydration of the coarser cement (Table 2) still lags far behind that of the finer cement, 0.83 vs. 0.95. This suggests that in conventional concretes, the finer cements definitely offer a performance benefit in terms of an enhanced degree of hydration.

3.3. Capillary porosity percolation

The percolation properties of the phases in cement paste have been examined previously using a computer model [19]. In that initial study based on a simple model of C_3S hydration only, a percolation threshold of about 18% was identified for the capillary porosity phase. Using the most recent version of the NIST microstructural model, Fig. 4 presents results for the two different cement PSDs at the three different w/c ratios examined in this study. One can clearly see that the cement PSD has a significant effect on the capillary porosity at which depercolation occurs. This topic is being explored further in current research and will be the topic of an upcoming paper [20]. With a coarser cement, the average interparticle spacing is larger, so that more hydration is needed to close off the capillary porosity. The effects of PSD are much greater than those of w/c ratio. For the w/c = 0.5, PSD = 30-μm system, the model is unable to hydrate the cement sufficiently to achieve depercolation of the capillary porosity. But even in this case, the percolation curve is asymptotically approaching those of the two lower w/c ratios. In general, the percolation threshold for the 30-μm systems is about 18%, while that for the 5-μm systems is about 22%. For the w/c = 0.5 systems, the effects of flocculation/dispersion on the capillary porosity percolation were negligible, as the data sets for the dispersed systems (not shown) basically overlapped those shown for the flocculated ones in Fig. 4.

Previously, this depercolation has been discussed in terms of the "curability" of the concrete [8]. In a cement paste, once the capillary porosity depercolates, the imbibition of water to replace that lost due to chemical shrinkage during hydration slows significantly [21], as transport shifts from being dominated by the capillary pores to being controlled by the much smaller gel pores in the C-S-H. Thus, the longer it takes for the capillary porosity to disconnect, the more time is available for additional water to diffuse into the interior of the concrete. For example, for the w/c = 0.3 cement pastes, depercolation occurs after 32 h (degree of hydration = 0.44) and 250 h (degree of hydration = 0.49) of hydration for the 5- and 30-μm systems, respectively, implying an increased curability for the coarser cement systems. This change in percolation threshold could also have significant effects on diffusivity and chemical shrinkage in these systems, as will be investigated in the following two sections.

3.4. Diffusivity

When evaluating the diffusivity properties of cement pastes of widely varying cement PSDs, one must be careful to separate hydration kinetics effects from microstructural effects. For example, Fig. 5 shows a plot of relative diffusivity coefficients (the diffusion coefficient of an ion in the concrete relative to its value in free water [15]) vs. hydration time. Because the finer cement hydrates much more rapidly, for a given w/c ratio its relative diffusivities are much lower at early times (<300 h). Eventually, for the lower w/c ratios hydration of the coarser cement will catch up with that of the finer one, and the two relative diffusivities will be nearly identical.

To separate the microstructural effects, the relative diffusivities are plotted against a microstructural parameter (total capillary porosity) in Fig. 6. Here, one can examine the effects of cement PSD on diffusivity from a microstructural viewpoint. For capillary porosities above the percolation threshold, one observes that the relative diffusivities of the coarser cements are about twice those of the finer cements

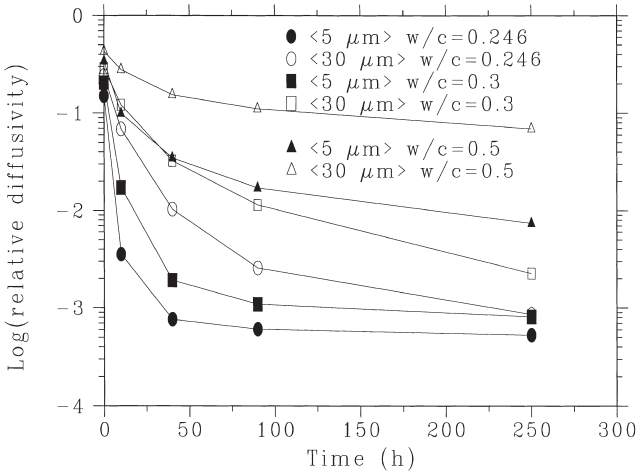

Fig. 5. Modeled relative diffusivity vs. hydration time for the six cement paste systems.

at the same porosity. This is most likely due to the larger pores present in the coarser cement systems. Although diffusivity is not directly dependent on pore size, it is inversely proportional to pore tortuousity, which will be decreased, and directly proportional to pore connectivity, which will be increased in the systems with larger pores.

This can be verified in Fig. 4 where the connected fraction of the porosity for each coarser cement always lies above that of the corresponding w/c ratio finer cement. After the capillary porosity depercolates, the relative diffusivities of the different systems are much more similar, with all approaching a limiting value of about 0.0004 at very low porosities.

The general shape of the curve fitted to the data in Fig. 6 is similar to that developed previously by Garboczi and Bentz [15]. Specifically, the relationship between relative diffusivity (D/D_0) and capillary porosity (ϕ) is given by Eq. (1):

$$\frac{D}{D_0} = 0.0004 + 0.03 \cdot \phi^2 + 3.0 \cdot (\phi - 0.20)^2 \cdot H(\phi - 0.20) \quad (1)$$

where $H(x)$ is the Heaviside function, taking values of 1 when $x > 0$ and 0 otherwise, and 0.20 represents the "average" percolation threshold for the capillary porosity. Eq. (1) was developed based on percolation concepts [15], with the three terms representing the inherent diffusivity of a C-S-H gel-unhydrated cement mixture (porosity = 0), the contribution of a depercolated capillary porosity network dispersed in a continuous C-S-H gel network, and the contribution of a percolated capillary pore network, respectively. The fitted equation is seen to provide a reasonable fit to the model data, as nearly all of the data points lie within the 2x bounds.

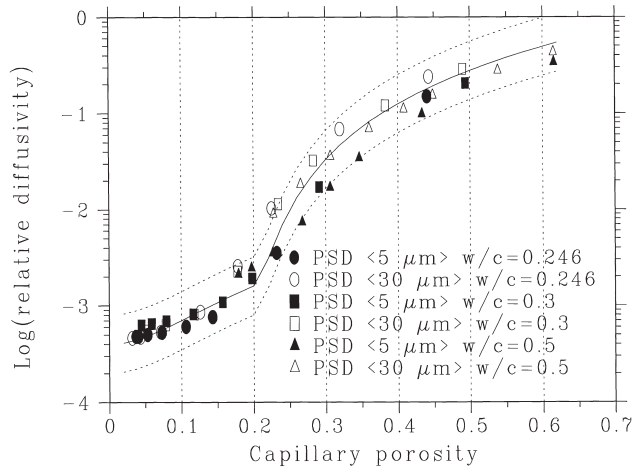

Fig. 6. Modeled relative diffusivity vs. total capillary porosity for the six cement paste systems. Solid line is the fitted function and dashed lines represent a factor of two above and below the fitted function.

3.5. Chemical shrinkage, internal relative humidity evolution, and autogenous shrinkage

As cement hydrates, the volume occupied by the hydration products is less than that of the reactants [6,21]. Thus, unless water is supplied from an external source, this chemical shrinkage will result in the formation of empty pores within the cement paste microstructure. This empty porosity not only influences the hydration kinetics [13] but also results in a reduction in internal relative humidity (RH) and a measurable autogenous shrinkage of the material [22]. Because this shrinkage generally occurs during the early life of the concrete, it often results in cracking and a loss of performance.

Because chemical shrinkage is directly proportional to degree of hydration [9,21], cement fineness will influence the time evolution of this property via its influence on hydration kinetics. In a totally sealed curing environment, the chemical shrinkage will result in the creation of empty porosity from time zero (or once set is achieved). At a fixed time, this chemical shrinkage will be much greater in the finer cement PSD system due to its enhanced hydration rate at early times. However, from a microstructural viewpoint, at equal degrees of hydration, the chemical shrinkage of the two systems will be identical.

Additionally, when curing under saturated conditions, cement fineness will influence chemical shrinkage through its influence on the depercolation of the capillary pore space, the point at which empty porosity will start to be formed within the material. Table 2 summarizes the empty porosity present in the systems examined in this study after 5,000 cycles of hydration. Because the finer cement depercolates and changes to "sealed" curing at a higher porosity (less hydration), its ultimate values of empty porosity are greater than those of the coarser cement, even when their degrees of hydration are similar.

For comparison, Table 2 also includes an entry for the w/c = 0.3, PSD = 30 μm system for hydration under totally

sealed conditions. In this case, not only is the final empty porosity fraction much greater, but the effects of curing under sealed conditions on the ultimate degree of hydration are also apparent [13]. Since hydration can no longer take place in the empty porosity, a substantial reduction in the ultimate degree of hydration is observed relative to that obtained for saturated curing.

Another effect of the chemical shrinkage is a reduction of the internal RH. As chemical shrinkage progresses, smaller and smaller pores become empty. Neglecting the effects of dissolved salts on RH, the size of the largest remaining water-filled pore will determine the local internal RH, according to the Kelvin-Laplace equation [13], as seen in Eq. (2):

$$\ln\frac{RH}{100} = -\frac{2V_m\gamma}{rRT} \tag{2}$$

where V_m is the molar volume of water, R is the universal gas constant, T is the temperature in Kelvin, γ is the surface tension of water, and r is the largest pore radius still filled with water. This analysis implies that in two systems with equivalent total porosities and equivalent amounts of chemical shrinkage, the one with the smaller pores will exhibit a much greater reduction in internal RH [23]. Thus, one would expect to observe a greater RH reduction when using a finer cement. Experimental results for two cements of the same clinker ground to two moderately different finenesses, which exhibit this behavior, are shown in Fig. 7 [24].

The chemical shrinkage occurring within the cement paste microstructure results in a measurable physical autogenous shrinkage of a much lower magnitude. Similar to the case of drying shrinkage [25], the magnitude of the autogenous shrinkage is proportional to the amount of water in tension within the microstructure and the capillary stress developed in the water [26]. Of course, the constant of proportionality will change with time due to hydration of the cement and creep of the C-S-H gel. The capillary stress, $\sigma_{capillary}$, is given by Eq. (3) [13]:

$$\sigma_{capillary} = -\frac{\ln\left(\frac{RH}{100}\right)RT}{V_m} \tag{3}$$

According to Eq. (3), the capillary stress in a cement paste produced with a fine cement will be greater due to its lower internal RH. For example, the capillary stress in a system with an internal RH of 70% will be seven times greater than that in a system with an internal RH of 95%.

Thus, there are two conflicting effects of cement fineness on autogenous shrinkage. On the one hand, a finer cement results in a greater RH reduction, resulting in higher values of the capillary stress. On the other hand, as illustrated in Table 2, the amount of water-filled porosity may be less in the finer cement paste due to its higher amount of chemical shrinkage and empty porosity when cured under the saturated conditions employed in this study. Because of the strong sensitivity of capillary stress to RH reduction, one would expect that in most cases of practical importance, the former effect would be dominant and a greater amount of autogenous shrinkage would be observed in the finer cement systems. Fig. 8 shows the equivalent autogenous shrinkage measurements (measured using a specially designed dilatometer placed in a constant temperature oil bath [24]) for the two systems whose RH evolutions were provided in Fig. 7 [24]. Indeed, in this case, the autogenous shrinkage observed for the finer cement is greater than that exhibited by the coarser cement. Taken together, these results suggest that under adequate curing conditions, the performance of coarser cements should be superior to finer cements with respect to the development of autogenous shrinkage and the early cracking that it often causes.

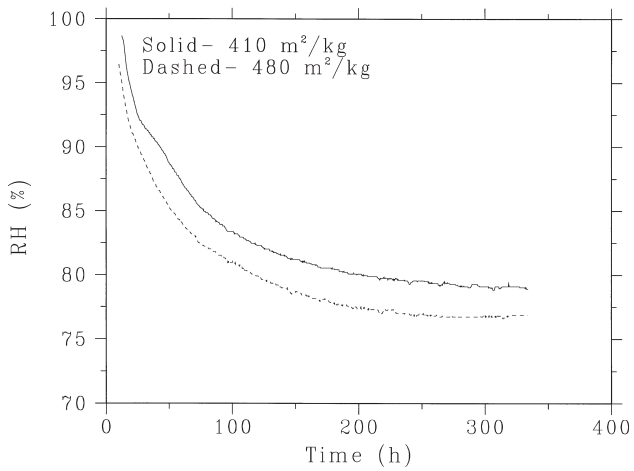

Fig. 7. Internal RH evolution vs. time for cements ground to two different finenesses, w/c = 0.30, 20% silica fume, 30°C [24].

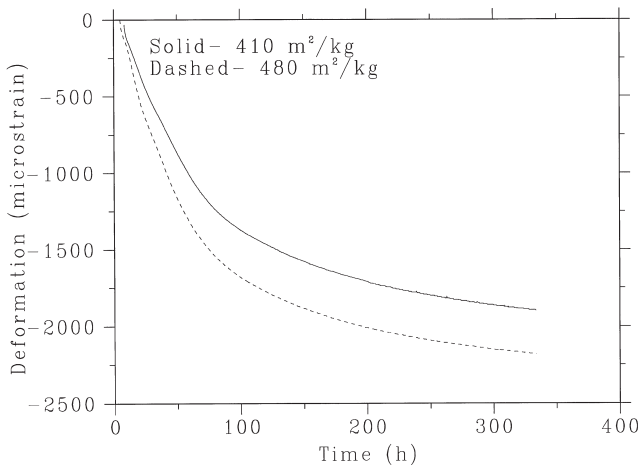

Fig. 8. Autogenous shrinkage evolution vs. time for cements ground to two different finenesses, w/c = 0.30, 20% silica fume, 30°C [24].

3.6. Interfacial transition zone microstructure

The final property examined as a function of cement PSD is the microstructure of the interfacial transition zone (ITZ). Initial two-dimensional microstructural images for the three-dimensional model are shown in Fig. 9 for the four systems investigated in this study. One can clearly observe differences in the packing efficiency near the aggregate surface for the different w/c ratios and cement PSDs. Since the thickness of this zone generally scales as the median cement particle diameter [27], one would expect to observe major differences between the two cement PSDs examined in this study. Indeed, this is the case for the w/c = 0.5 systems, as shown in Fig. 10, which plots the initial and final (after 5,000 cycles of model hydration or about 25,000 h) porosity distributions for the two different cements. For the coarser cement, one can clearly observe an increased porosity in the ITZ region. This increased porosity would generally have detrimental effects on both the mechanical properties and transport coefficients of the concrete. For diffusivity, this effect is fairly small, but for permeability, it could be significant [28].

However, as illustrated in Fig. 11, for the w/c = 0.3 systems, the differences in the porosity distributions of the two systems are relatively similar after the 5,000 cycles of hydration. One interesting feature of this graph is the appearance of a small local maximum in the porosity distribution for each hydrated system at a distance of about five pixels from the aggregate interface. The cause of this feature is the chemical shrinkage and self-desiccation occurring during hydration (after the capillary porosity depercolates), as verified by examining two-dimensional images of the microstructure after hydration. In the model, the largest pores are the first to empty during self-desiccation. In a system with an aggregate particle, the largest pores are generally those closest to the aggregate surface so that a large fraction of the empty porosity forms in the ITZ region. This is particularly true in the case of the coarser cement. This observation is consistent with direct microstructural measurements performed using scanning electron microscopy [29], where relatively large pores are observed in the ITZ regions. In the past, these pores have been attributed to hollow-shell hydra-

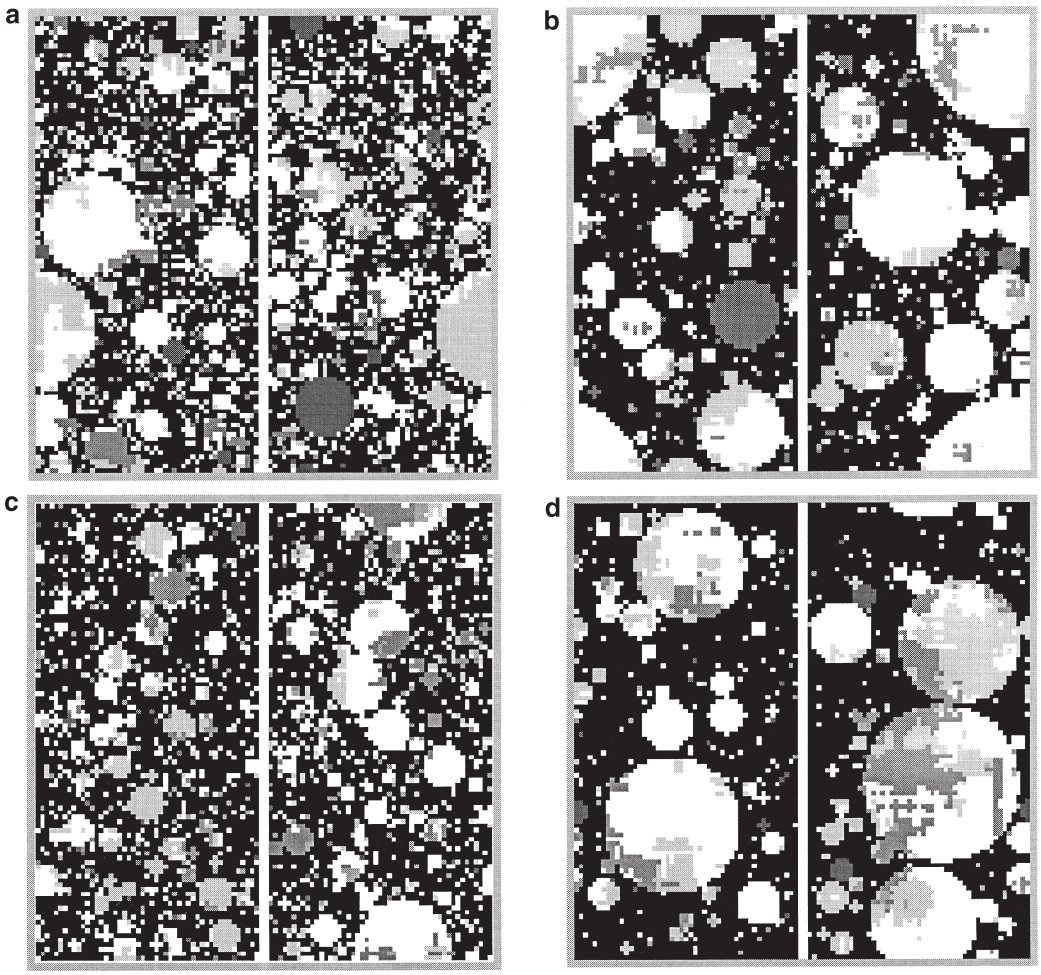

Fig. 9. Original microstructure images for: (a) w/c = 0.3, PSD = 5 μm; (b) w/c = 0.3, PSD = 30 μm; (c) w/c = 0.5, PSD = 5 μm; and (d) w/c = 0.5, PSD = 30 μm. Phases from brightest to darkest are: C_3S, C_2S, C_3A, C_4AF, hemihydrate, and porosity. Central white bar extending across the microstructure is the flat plate aggregate.

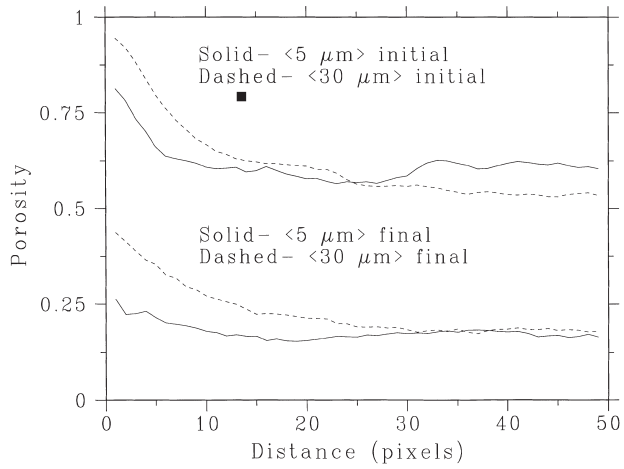

Fig. 10. Porosity fraction vs. distance from aggregate surface for w/c = 0.5 model cement pastes.

tion (Hadley) grains [30] or to the dissolution of calcium hydroxide crystals in systems containing silica fume [29], but they could also be the result of self-desiccation in lower w/c ratio mortars and concretes.

4. Conclusions

Based on modeling and a few experimental studies, the following preliminary conclusions can be drawn with respect to the effects of cement PSD on performance properties:

- Setting time: Coarser cements will require more time to achieve set, although they actually achieve set at a lower degree of hydration. Their strength development will also lag significantly behind that of finer cements.
- Heat release: Coarser cements will result in a lower initial heat release rate, which could be useful when thermal cracking is a concern.

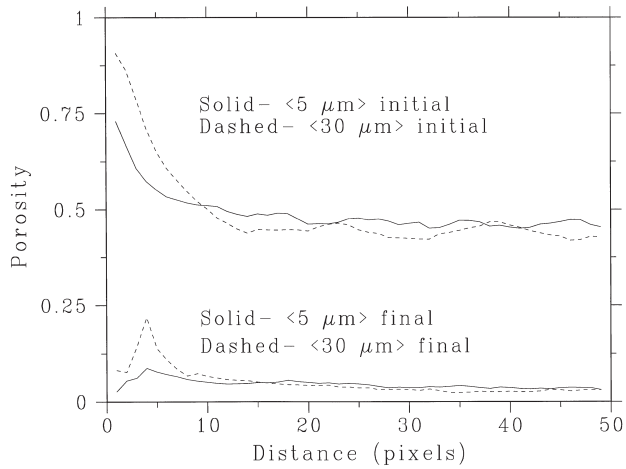

Fig. 11. Porosity fraction vs. distance from aggregate surface for w/c = 0.3 model cement pastes.

- Capillary porosity percolation: Coarser cements require more hydration for the capillary porosity to depercolate, implying a possibly enhanced curability.
- Diffusivity: At equivalent times, the diffusion coefficients for the coarser cements are much higher than those for the finer cements. At equivalent degrees of hydration, the diffusion coefficients of the coarser cements are still about a factor of two greater than those of the finer cements before depercolation of the capillary porosity and approximately equivalent thereafter.
- Chemical shrinkage: Under proper and carefully controlled curing conditions, less empty porosity should be created in the systems based on the coarser cements.
- Internal RH evolution and autogenous shrinkage: The reduction in internal RH will be less for the coarser cements. Although they may contain more water-filled porosity, the coarser cements will also generally produce less autogenous shrinkage.
- ITZ microstructure: For conventional w/c ratios, the coarser cement results in an ITZ microstructure characterized by a higher porosity and larger pores. At low (0.3) w/c ratios, this effect becomes less significant.

For the w/c = 0.5 systems, a study of cement particle flocculation/dispersion indicated that only the setting characteristics were significantly influenced by this parameter. For the dispersed systems, more time and more hydration were needed to achieve set. In this study, capillary porosity depercolation, chemical shrinkage, and relative diffusivity were found to be relatively unaffected by the flocculation state of the initial microstructures.

In all of the simulations, “ideal” curing conditions were utilized. Coarser cements will require more attention to be paid to curing in the field, to achieve their full potential. If adequate curing cannot be guaranteed, the finer cements are preferable due to both their increased early hydration rate and their earlier depercolation of the capillary porosity (which minimizes water loss). While no one cement particle size distribution is ideal for all applications, the cement PSD can be optimized for each particular application.

The purpose of this study has been to point out the advantages of carefully considering cement fineness when designing concrete for a specific task. The power of using a combined experimental/microstructural modeling approach to this problem has been demonstrated and will be developed further in future cooperative research (including experimental studies of autogenous shrinkage and internal stress development for the “model” cements considered in this study).

References

[1] G. Frigioine, S. Marra, Relationship between particle size distribution and compressive strength in Portland cement, Cem Concr Res 6 (1976) 113–128.
[2] B. Osbaeck, V. Johansen, Particle size distribution and rate of

strength development of Portland cement, J Am Ceram Soc 72 (2) (1989) 197–201.
[3] J.M. Pommersheim, Effect of particle size distribution on hydration kinetics. in: Materials Research Society Symposium Proceedings, 85, L.J. Struble, P.W. Brown (Eds.), Mat Res Soc, Pittsburgh, 1987, pp. 301–306.
[4] T. Knudsen, The dispersion model for hydration of Portland cement I. General concepts, Cem Concr Res 14 (1984) 622–630.
[5] S. Wakasugi, K. Sakai, S. Shimobayashi, H. Watanabe, Properties of concrete using belite-based cement with different fineness, in: O.E. Gjorv (Ed.), Concrete under Severe Conditions 2, E & FN Spon, London, 1998, pp. 2161–2169.
[6] H.F.W. Taylor, Cement Chemistry, 2d ed., Thomas Telford, London, 1997.
[7] P.K. Mehta, Durability—Critical issues for the future, Concr International 19 (7) (1997) 27–33.
[8] D.P. Bentz, C.J. Haecker, An argument for using coarse cements in high performance concrete, Cem Concr Res 29 (1999) 615–618.
[9] D.P. Bentz, Three-dimensional computer simulation of Portland cement hydration and microstructure development, J Am Ceram Soc 80 (1) (1997) 3–21.
[10] D.P. Bentz, Guide to using CEMHYD3D: A three-dimensional cement hydration and microstructure development modelling package, NISTIR 5977, U.S. Department of Commerce, February 1997, software and manual available over the Internet from anonymous ftp at ftp.nist.gov (129.6.13.25) in the /pub/bfrl/bentz/CEMHYD3D subdirectory and described in electronic monograph online at http://ciks.cbt.nist.gov/garboczi/.
[11] D.P. Bentz, unpublished results, 1998.
[12] A. Nonat, Interactions between chemical evolution (hydration) and physical evolution (setting) in the case of tricalcium silicate, Mater Struct 27 (1994) 187–195.
[13] D.P. Bentz, K.A. Snyder, P.E. Stutzman, Microstructural modelling of self-desiccation during hydration, in: B. Persson, G. Fagerlund (Eds.), Self-Desiccation and Its Importance in Concrete Technology, Lund Institute of Technology, Lund, Sweden, 1997, pp. 132–140.
[14] E.J. Garboczi, Finite element and finite difference programs for computing the linear electrical and elastic properties of digital images of random materials, NISTIR 6269, U.S. Department of Commerce, December, 1998, and described in electronic monograph available online at http://ciks.cbt.nist.gov/garboczi/.
[15] E.J. Garboczi, D.P. Bentz, Computer simulation of the diffusivity of cement-based materials, J Mat Sci 27 (1992) 2083–2092.
[16] G. Fagerlund, Effect of self-desiccation on the internal frost resistance of concrete. in: B. Persson, G. Fagerlund (Eds.), Self-Desiccation and Its Importance in Concrete Technology, Lund Institute of Technology, Lund, Sweden, 1997, pp. 227–238.
[17] D.P. Bentz, V. Waller, F. de Larrard, Prediction of adiabatic temperature rise in conventional and high-performance concretes using a 3-D microstructural model, Cem Concr Res 28 (2) (1998) 285–297.
[18] W.G. Lei, Rheological studies and percolation modeling of microstructure development of fresh cement paste, Ph.D. Thesis, University of Illinois, Urbana-Champaign, IL, 1995.
[19] D.P. Bentz, E.J. Garboczi, Percolation of phases in a three-dimensional cement paste microstructural model, Cem Concr Res 21 (2/3) (1991) 325–344.
[20] E.J. Garboczi, D.P. Bentz, Re-examination of the capillary porosity percolation of a cement paste microstructural model, to be submitted to Cem. Concr. Res.
[21] M. Geiker, Studies of Portland cement hydration: Measurements of chemical shrinkage and a systematic evaluation of hydration curves by means of the dispersion model, Ph.D. Thesis, Technical University of Denmark, Lyngby, 1983.
[22] C. Hua, P. Acker, A. Erlacher, Analyses and models of the autogenous shrinkage of hardening cement paste, I. Modelling at the macroscopic scale, Cem Concr Res 25 (7) (1995) 1457–1468.
[23] O.M. Jensen, P.F. Hansen, Autogenous deformation and change of the relative humidity in silica fume modified cement paste, ACI Mat J 93 (6) (1996) 539–543.
[24] O.M. Jensen, Influence of cement type upon autogenous deformation and change of the relative humidity, Technical Note, Technical University of Denmark, 1995.
[25] V. Baroghel-Bouny, Experimental investigation of self-desiccation in high-performance materials—Comparison with drying behavior, in: B. Persson, G. Fagerlund (Eds.), Self-Desiccation and Its Importance in Concrete Technology, Lund Institute of Technology, Lund, Sweden, 1997, pp. 72–87.
[26] D.P. Bentz, E.J. Garboczi, D.A. Quenard, Modelling drying shrinkage in porous materials using image reconstruction: application to porous Vycor glass, Mod Sim Mat Sci Eng 6 (1998) 211–236.
[27] D.P. Bentz, E. Schlangen, E.J. Garboczi, Computer simulation of interfacial zone microstructure and its effect on the properties of cement-based composites, in: J.P. Skalny, S. Mindess (Eds.), Materials Science of Concrete IV, The American Ceramic Society, Westerville, OH, 1995, pp. 155–199.
[28] J.D. Shane, T.O. Mason, H.M. Jennings, E.J. Garboczi, D.P. Bentz, Effect of the interfacial transition zone on the conductivity of Portland cement mortars, accepted by J Am Ceram Soc, 1999.
[29] D.P. Bentz, P.E. Stutzman, Evolution of porosity and calcium hydroxide in laboratory concretes containing silica fume, Cem Concr Res 24 (6) (1994) 1044–1050.
[30] D.N. Hadley, The nature of the paste-aggregate interface, Ph.D. Thesis, Purdue University, West Lafayette, IN, 1972.